Atmósfera (1988), **1**, pp. 5-16

Spectral and total albedo to solar radiation of ice and water clouds - experimental results from ASPIRE

GARTH W. PALTRIDGE
CSIRO Division of Atmospheric Research, Private Bag Num. 1, Mordialloc, Victoria, 3195, AUSTRALIA

(Manuscript received August 4, 1987; accepted October 14, 1987)

RESUMEN

Un experimento extenso (the Aspendale ISCCP Regional Experiment) para estudiar las propiedades radiativas y microfísicas de nubes de fase mixta, produjo perfiles (obtenidos utilizando un avión) para 3 capas de cirrus completamente congelados, dos capas de estratocúmulus de agua líquida y 2 capas de altoestratocúmulus en fase mixta.

Los resultados para la radiación solar de onda corta se presentan aquí. Los espectros de reflexión en el rango de 1.1 a 2.5μm resultaron muy afectados por ruido instrumental, haciendo que los detalles de la absorción en el infrarrojo no pudieran ser examinados. Sin embargo los promedios más anchos de la reflectividad de las nubes, como función de la longitud de onda, resultaron consistentes con el trabajo teórico de Wiscombe *et al.* (1984). El análisis del albedo del espectro total A, obtenido con piranómetros Eppley, produjo relaciones bastante consistentes entre A y el trayecto total de agua o hielo W para ángulos centrales solares del orden de 60°: o sea

$$A = 0.07 + 0.037(log\, W)^2$$

para los estratocúmulus y

$$A = 0.0079(log\, W)^2$$

para los cirrus. El albedo para los altoestratos de fase mixta se localiza afortunadamente entre estos dos extremos, siendo aparentemente una función sencilla de la fracción de agua, con respecto al total. La inesperada consistencia de la relación para los cirrus se discute y se atribuye al aparentemente constante radio promedio de las partículas ($\approx 200\mu$m) de las nubes examinadas. Se propone una parametrización con el propósito de tomar en cuenta el radio efectivo promedio.

ABSTRACT

An extensive experiment (the Aspendale ISCCP Regional Experiment) to study the radiative and microphysical properties of mixed-phase clouds yielded aircraft profiles from 3 fully iced cirrus decks, 2 liquid water decks of stratocumulus and 2 mixed-phase decks of altostratus. The short-wave solar radiation results are presented here. The reflection spectra from 1.1 to 2.5μm suffered badly from instrumental noise and the detail of infrared absorption could not be examined. However, the broadest average of cloud reflectivity as a function of wavelength was consistent with the theoretical work of Wiscombe *et al.* (1984). Analysis of total spectrum albedo A as measured by Eppley pyranometers yielded fairly consistent relations between A and total water or ice path W for solar zenith angles of the order of 60°: namely,

$$A = 0.07 + 0.037(log\, W)^2$$

for the stratocumulus, and

$$A = 0.0079(log\, W)^2$$

for the cirrus. The albedo of the mixed-phase altostratus sat nicely between the two extremes as an apparently simple function of the fraction of liquid water to the total. The unexpected consistency of the cirrus relation is discussed and attributed to the relatively constant mean particle radius ($\approx 200\mu$m) of the clouds examined. A parameterization to take account of mean effective particle radius is proposed.

Introduction

The radiative characteristics of cloud depend in principle on a number of very complex factors which are not likely to be available (i.e. predicted or observed) on the global scale required for climate models. It is inconceivable for instance that the drop size distribution of water clouds or the particle size distribution of high level ice clouds will ever be measured or predicted in other than very

restricted experimental circumstances. The hope must be that the relevant radiative parameters can be calculated to sufficient accuracy from broader measures of cloud character. The most detailed information that is likely to be generally available apart from cloud geometry (height, thickness and fractional cover) is some average of total water or ice path in a given cloud deck, and perhaps some indication of mean particle size.

This paper reports experimental results on the reflectance and spectral reflectance to solar radiation of various cloud decks and the relation of that reflectivity to the total vertical water path. The results are part of the information obtained during an extensive 3-week experiment at Mildura, Australia, in June of 1985. The experiment was known colloquially as ASPIRE (the Aspendale ISCCP Regional Experiment) and involved the CSIRO F-27 research aircraft fully instrumented for radiative and cloud physics measurements, ground based lidar and infra-red radiometer, and direct access to HRPT and GMS satellite data. The basic intention was to examine the characteristics of middle-level mixed-phase (i.e. ice and water) clouds and it was this and the research aircraft ceiling ($\sim$ 7500 m) which dictated the choice of Mildura in winter. In the event the experiment provided usable data on three fully-iced cirrus decks, two mixed-phase decks of altostratus, and two decks of stratocumulus. They were all reasonably uniform cloud layers with no other cloud above or below to interfere with the interpretation of the radiation data.

The operational object (not often achieved) was to obtain the aircraft profiles of a given cloud as it passed over the ground-based lidar. The hope of timing this to coincide exactly with an overpass of the NOAA satellite was never realized.

Instrumentation and analysis

The full complement of instruments available to the overall ASPIRE experiment is summarized in Table 1. The following comments refer specifically to equipment relevant to the present analysis.

TABLE 1. Summary of Instrumentation deployed during ASPIRE (June 1985)

1. Radiation Equipment

Instrument	Time Constant	Sampling Rate	Wavelength Response	Comments
(i) Eppley Pyranometers	$\sim$ 10 sec.	$\sim$ 10 sec.$^{-1}$	0.285μm<λ<2.8μm	Upward and downward looking with hemispheric fields of view
(ii) Eppley Pyrgeometers	$\sim$ 10 sec.	$\sim$ 10 sec.$^{-1}$	4μm<λ<50μm	As per pyranometers
(iii) Infrared Radiometer	$\sim$ 5 sec.	$\sim$ 3.5 sec.	10μm<λ<12μm	Narrow field of view ($\sim$ 10mrad) either up or down looking - min. detectable radiance $\sim$ 0.03Wm^{-2}Sr^{-1}
(iv) Spectrally Scanning Radiometer (SPERAD)	>> 0.01 sec.	$\sim$ 10 spectra per sec.	0.4μm to 2.5μm	$\sim$ 20nm bandwidth, 7 mrad field of view, upward and downward looking (see text)
(v) Video Camera			Visible	200-line resolution over 60 degree field of view

2. Cloud Microphysics

Instrument-Particle Spectrometers	Particle Size (r)	Comment
PSSP	2<r<47μm	Knollenberg instruments from PMS of Boulder
OAP-200	300<r<4500μm	
2D Probe	25<r<800μm	

Table 1 (Continued)

3. Thermodynamics

Variable	Instrument	Response	Comment
Cloud Liquid Water	CSIRO King Hot Wire	∿100Hz	
Cloud Ice Water	CSIRO King Hot Wire	∿100Hz	See text
Dry Bulb Temperature	Rosemont	∿1Hz	
Wet Bulb Temperature	Rosemont	∿1Hz	
Pressure	Pitostatic Tube	∿10Hz	
Aircraft Air Speed	Pitostatic Tube	∿10Hz	

Note: These measurements supplemented by operational radiosonde data.

4. Other Variables from Inertial Navigation System (sampling rate ∿10 Hz)

Ground speed, pitch angle, roll angle, drift angle, magnetic heading, position latitude and longitude, true heading, inertial altitude, vertical acceleration, wind angle, wind speed.

5. Ground Based Instrumentation

Ruby Lidar - 0.694μm, energy 1 Joule, pulse length 60 n sec., repetition rate up to 1 per second.

Infra-red Radiometer - $10<\lambda<12\mu m$, min. detectable radiance $0.025 Wm^{-2}Sr^{-1}$, time constant 5 seconds.

The aircraft spectral radiometer (SPERAD - see Scott and Stephens, 1985) gave separate spectra of both the downcoming total solar flux and the vertical upward radiance - the latter with a beamwidth of 7 mrad. It produced spectra covering the wavelength range 400 nm to 2500 nm every eighth of a second. This corresponds roughly to every 10 meters in the horizontal for the typical aircraft speed of 80 meters per second. The instrument was calibrated prior to the experiment and the calibration was checked at the end. The total spectrum solar fluxes were obtained from upward and downward looking Eppley pyradiometers mounted respectively in a pod above the aircraft and in a bay in the lower fuselage. Their time constant was about 10 seconds.

The microphysical instrument detectors were disposed in various pods about the aircraft nose. The CSIRO designed ice-water probe (King and Turvey, 1986) was a modification of the hot-wire liquid water probe (King *et al.*, 1978 and 1985) also flown on this occasion. The ice-water probe was 'contaminated' by liquid water whenever liquid water was present, so that in the mixed-phase clouds the ice content was computed from the particle spectrum obtained by the Knollenberg spectrometers (see below). In this computation the assumption was made that the particles were spherical. The estimate of ice water content on these occasions was therefore an outside limit.

The aircraft carried three Knollenberg drop and particle size detectors manufactured by PMS of Boulder, Colorado. The first was a 2-D imaging probe which recorded the spectrum of particles in the size range 25 to 800 μm as well as actual 2-D images of the individual particles. The second was an Optical Array Precipitation spectrometer which records the size spectrum from 0.3 to 4.5 mm. The third was a forward scattering spectrometer designed to give the size distribution of water drops in the range 1 to 25 μm, but this instrument became unserviceable during the experiment so that no information was available on the spectra of water drops in the low-level water clouds. Rosemont equipment was used to monitor wet and dry bulb temperatures.

All data were recorded on magnetic tape and were locked in time to the output of a video recorder mounted so as to look downwards through a port in the lower fuselage. Voice communication and flight description were recorded on the sound track of the same recorder.

For the present purpose the SPERAD radiometer spectral data were averaged over 20-second periods so as to be roughly compatible with the 10 second time constant of the Eppley pyranometers. Up to ten of these periods, each corresponding to a different level, were abstracted from each ascent or descent through a cloud.

The basic radiative parameter of concern in the present work is cloud albedo - either the albedo A to the total spectrum of solar radiation as measured by the Eppley pyranometers or the spectral albedo A_λ to a particular short wavelength λ as measured by the SPERAD. Furthermore the concern is with albedo of the layer to a uni-directional flux (i.e. to the downcoming radiation). All the measured radiation profiles contain components derived from flux impinging on both the top and bottom of the cloud layer, and calculation of the uni-directional reflectance or albedo from actual measurements requires a certain amount of assumption and approximation.

The downward solar flux at the top of a cloud is primarily direct-beam radiation. Let the parenthesized z_o and z indicate values of quantities at cloud top and depth z respectively, let a be the absorptance and A the albedo of the layer of cloud from z_o to z, and let $\overline{A}$ be the albedo of this layer to upwelling diffuse solar radiation reflected from cloud and atmosphere and ground below z. Thus

$$M^+(z) = (1 - a - A)M^+(z_o) + \bar{A}M^-(z) \tag{1}$$

an

$$M^-(z_o) = (1 - a - \bar{A})M^-(z) + AM^+(z_o) \tag{2}$$

where the M are the short-wave flux densities in the downward (+) or upward (-) directions, and it is assumed that the same fraction a is absorbed of both the upwelling and downcoming fluxes. (This approximation is discussed shortly).

The equations can be solved to give an expression for A which, unfortunately, contains the diffuse albedo $\overline{A}$. In principle one could derive a theoretical relation between A and $\overline{A}$ as a function of solar zenith angle and thereby obtain a unique expression for A in terms only of the measured flux densities. However the assumptions required would not necessarily yield a result more reliable than that based on the simple approximation actually used here - namely that $\overline{A} = A$ at the solar zenith angles of the present measurements which were all close to about 60^o (see Table 2).

Using that approximation equation (1) can be re-arranged to give

$$A = \frac{M^+(z_o)(1 - a) - M^+(z)}{M^+(z_o) - M^-(z)} \tag{3}$$

Once one accepts the approximation that $\overline{A} = A$ at the solar zenith angles of the present measurements, it is possible to generalize equation (3) such that z_o can be any level (z_1 say) in the cloud deck and z is any level below z_1.

There is difficulty with regard to the absorptance a. In principle it can be calculated by solution of equations (1) and (2) as

$$a = \frac{[M^+(z_1) - M^-(z_1)] - [M^+(z) - M^-(z)]}{M^+(z_1) + M^-(z)} \tag{4}$$

The following discussion refers first to wide-band (i.e. total spectrum) absorption.

Since water vapour contributes an arguable but very large fraction of cloud absorption and since water vapour absorption tends to saturate at values of the order of 0.15 at quite small water vapour path lengths (e.g. Paltridge, 1973), the absorption of upwelling radiation and the absorption of downcoming radiation in at least the lower levels of a cloud should be very small. This tends to negate the assumption of equations (1) and (2) (i.e. that a is the same for both upwelling and downcoming radiation) so that the values of a calculated from equation (4) are theoretically doubtful. Furthermore, the experimental error associated with the measurement of a in clouds (equation (4) involves small differences of large quantities) is very large. Thus, for the present calculations of total spectrum albedo via equation (3), a has been set at a constant 0.1 for all cloud layers z_1 to z for both ice particle cloud layers and water drop cloud layers. This is a somewhat arbitrary procedure, but for what it is worth this value of 0.1 is close to the average of the absorptance calculated via equation (4) for all the layers considered here.

One of the instrumental failures of the experiment concerned the SPERAD measurement of the infrared part of the downcoming shortwave spectrum (i.e. from 1.1 to 1.5 μm). There was sufficient electrical noise on the relevant detector to make accurate measurement at individual wavelengths of the downcoming IR impossible. The best that could be done was to derive the general slope, and as a consequence any calculated spectral albedo in the infrared (using the spectral version of equation (3) and the spectral measurements of SPERAD) is little more than a qualitative indication. The failure was very unfortunate since it is effectively impossible to analyse (for instance) the effect of infrared absorption on albedo.

Figure 1 gives the observed spectra of *upcoming* radiance in three situations. That is, at the mid-level of the thickest cirrus deck (flight 3), at the mid-level of the stratocumulus deck of flight 9, and at an altitude of 2000 meters in the perfectly clear sky observed during flight 14. The total water path from the top of the atmosphere (i.e. from the aircraft maximum altitude of 7500 meters where the humidity was invariably so low as to be unmeasurable by the Rosemont instrumentation) down to the relevant level is given for each spectrum in the caption to the figure. The radiance axis is different in the case of the cirrus. It has been chosen so that all three spectra have a common point on the graph at the non-absorbing wavelength of 650 nm. That is, the spectra have been graphically normalized at that point.

The clear-sky radiance at wavelengths shorter than 650 nm is less than the radiance in the clouds because (presumably) of the chlorophyll absorption at these wavelengths by the vegetation cover of the ground. In the infrared region of the spectra are the obvious 'valleys' of the major water vapour (and liquid water and ice) absorption bands at 0.95, 1.15, 1.35 and 1.85 μm. Between 'the valleys' the upcoming radiance is relatively less in the clouds than in the clear sky which, provided that radiation scatter is not greatly dependent on wavelength over this range, is an indication of significant infrared absorption by water particles in spectral regions where water vapour absorption is very small. (See also Irvine and Pollack, 1968; Hale and Query, 1973).

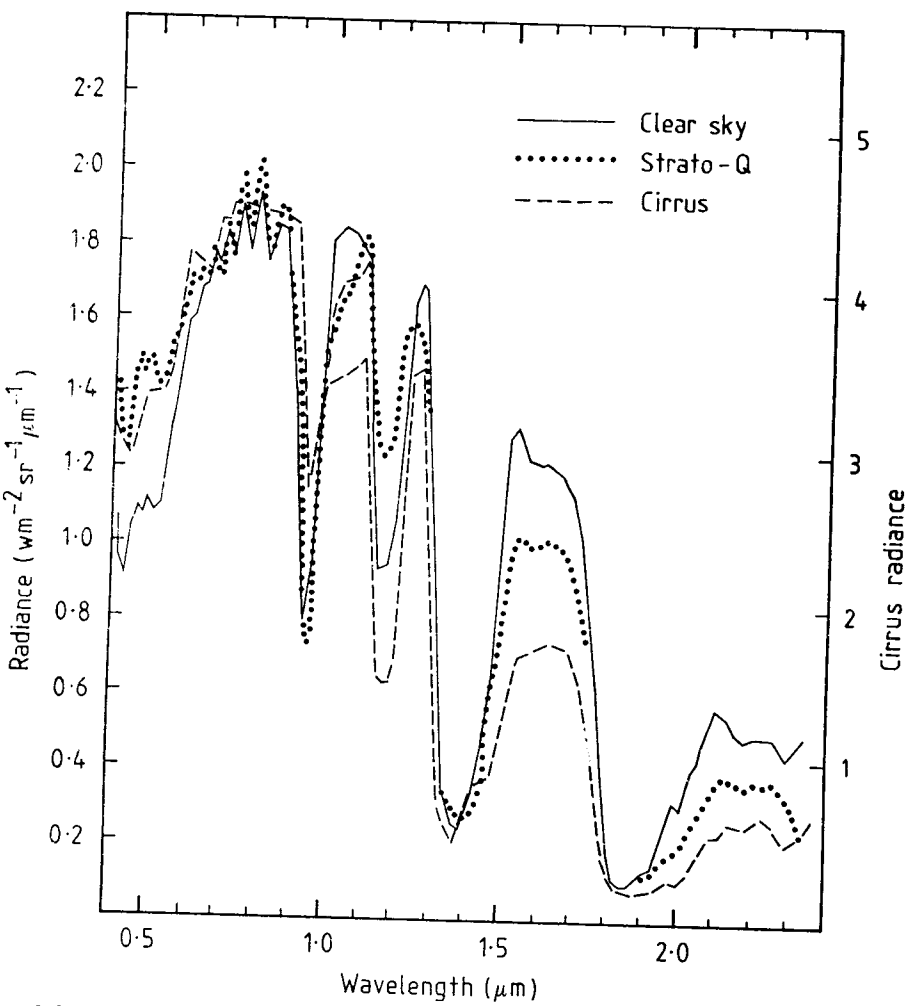

Figure (1). Examples of the spectra of upcoming short-wave radiance obtained (1) at the mid-level of the stratocumulus of flight 9 where the total water path from the top-of-atmosphere (TOA) was 17.5 g. m^{-2}, (2) at the mid-level of the cirrus deck of flight 3 where the water path from TOA was 1100 g. m^{-2}, and 3 at an altitude of 2000 m in the clear sky of flight 14 where the total water path from TOA was 0.56 g. m^{-2}. The scale of the cirrus radiance has been expanded for ease of comparison of the shapes of the infrared absorption bands (see text).

As mentioned above, the noise on the downcoming infrared spectra allows only the broadest average spectral albedo to be calculated. Figure 2 is a plot of average normalized spectral albedo or reflectance calculated according to the spectral version of equation (3) for those wavelengths *outside* the major absorption 'valleys'. The curve is the average of 25 sub-layers of cloud obtained from the seven cloud decks recorded in Table 2. Each sub-layer extends from some depth z_1 (usually cloud top) down to some other depth z, so they are not completely independent. The spectral albedo of each sub-layer was normalized to a common value of 0.5 at 650 nm, and the error bars are the range of normalized reflectances at each wavelength. Note that the normalization allows some reflectance values to exceed 1.0.

The main point of the graph is to show that, when sufficient averaging is performed to 'overcome' the instrumental noise problem mentioned earlier, there is a fair correspondence in shape of the reflectance spectrum to that theoretically calculated by Wiscombe *et al* (1984). Their curve (again

normalized here to 0.5 at 650 nm) is the dashed line in Figure 2. It is an interpolation of their results for large-droplet *water* clouds for solar zenith angles of 0^o and 78^o to the 60^o of the present measurements.

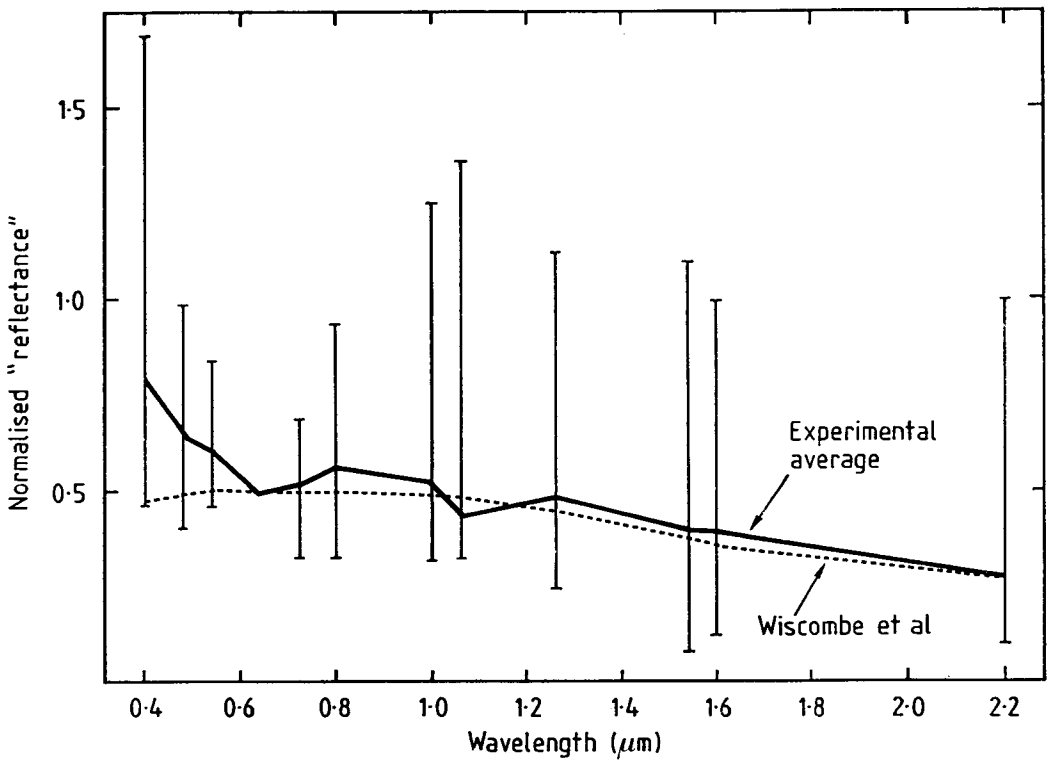

Figure (2). Average normalized reflection spectrum obtain from 25 semi- independent layers of *all* clouds examined (i.e. both ice and water clouds). Points obtained at wavelengths outside the major absorption bands. Normalization (to 0.5 at 650 nm) performed on all individual spectra before averaging. The dashed curve is the theoretical calculation of Wiscombe et al. (1984) for their large water drop cloud.

TABLE 2 - Basic data on cloud decks over Mildura analysed from ASPIRE (June 1985)

Date	Time (Profile mid-point)	Flight Number	Cloud Top(m)	Cloud Base(m)	Mid-level Temperature (K)	Average Liquid Water $g.m^{-3}$	Average Ice Water $g.m^{-3}$	Average Ice Particle No. Density l^{-1}	Total Water Path $g.m^{-2}$ (top to base)	Average Air Mass	Type
9/6/85	12.25hrs	3	6960	3000	258	0	.5	10	2000	1.84	Cirrus
13/6/85	11.50hrs	8	1520	1270	278	.15	0	?	34	1.91	Stratocumulus
14/6/85	11.05hrs	9	1370	1050	275	.09	0	?	27	2.03	Stratocumulus
17/6/85	14.40hrs	11A	7550	6050	245	0	.12	4	195	2.30	Cirrus
	15.05hrs	11B	7550	6050	245	0	.06	2	74	2.48	Cirrus
18/6/85	13.15hrs	12A	3650	2600	269	.05	.15	.5	210	1.95	Altostratus
	14.05hrs	12B	3700	1900	270	.20	.60	1	1400	2.25	Altostratus
20/6/85	10.21hrs	14	Total water vapour path ground to 4000m = .79 gm^{-2}								Clear sky

Total spectrum albedo

The rest of the paper deals with the total albedo measurements by the broad-band Eppley pyranometers. Again individual albedo values were obtained for several sub-layers of each cloud deck - i.e. from cloud top to several different depths within the cloud, and also from several depths within the cloud to the cloud base. It is worth repeating that the calculations assume an equality of diffuse and direct beam albedos at the solar zenith angles of the present measurements (i.e. about 60°).

Thus, the albedos as a function of vertical water path are plotted in Figure 3. The three categories of cloud (ice, liquid water, and ice and liquid water) are shown as different symbols.

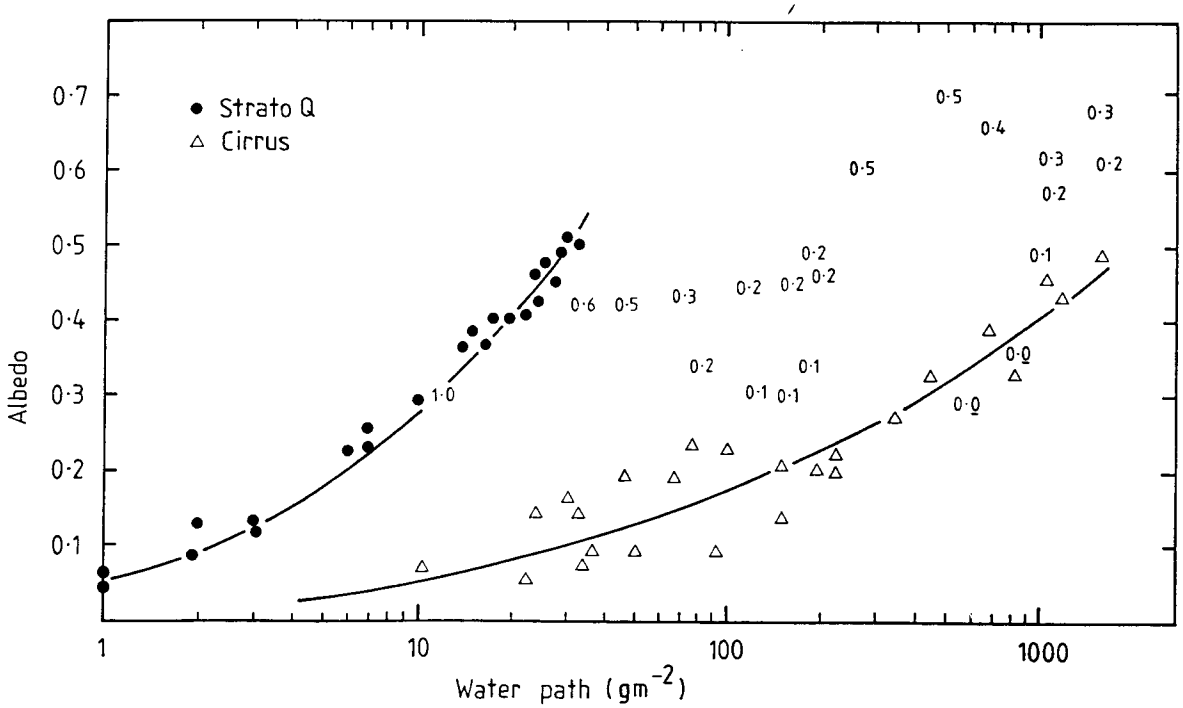

Figure (3). Measured total short-wave albedo as a function of water or ice path for stratocumulus (the dots), cirrus (the triangles) and mixed-phase altostratus (the decimal numbers). The decimal fraction refers to the fraction of liquid water in the total water path. The lines of best fit are quoted in the text.

It is obvious and expected that ice clouds and water clouds have an entirely different albedo versus water path relation. They are surprisingly consistent within themselves and the best fit curves over the measured range of water paths are as follows:

$$A = 0.07 + 0.037(\log W)^2 \tag{5a}$$

for the stratocumulus water clouds, and

$$A = 0.0079(\log W)^2 \tag{5b}$$

for the cirrus ice clouds, where the correlation coefficients are 0.98 and 0.94 respectively. (Note that the relations concern clouds where the solar zenith angle is confined to a fairly narrow range about 60°). The numbers on the graph refer to measurements in the two mixed-phase altostratus clouds.

(The relevant microphysical information and some discussion concerning these particular clouds is to be given in a separate paper. It need be noted here that there was a thin layer of pure liquid water at the top of each cloud, with glaciation increasing toward cloud base). The numbers on the graph are the fraction f of liquid water to total water in the vertical path and can be regarded as graphical symbols. There is a quite smooth progression of the value of f from the ice cloud line ($f = 0$) to the liquid water line ($f = 1.0$) - smooth enough at any rate to accept as a first approximation that there is a steady progression in albedo from ice to water clouds as a function of f.

Discussion

The geometrical scattering cross-section X of all the drops in a given cloud liquid water path W decreases as the mean effective radius $\bar{r}_e$ increases. This is because the cross-section of a single drop increases as the square of its radius while the number density of drops (since W is fixed) decreases in inverse proportion to $\bar{r}_e^3$. That is,

$$X \quad \propto \quad 1/\bar{r}_e. \tag{6}$$

However, the scattering *efficiency* of drops increases with radius until it reaches the maximum value at size parameters of the order of 10 to 20 - that is, in the case of short-wave radiation, when the drops reach about 2 to 5 μm radius. Albedo depends on the product of geometrical scattering cross-section and scattering efficiency. Therefore it is to be expected that, for typical stratocumulus where the drop sizes are not excessively large, the albedo is more or less independent of $\bar{r}_e$ and of drop-size distribution and depends only (primarily?) on liquid water path. The theoretical work of Chýlek (1978) suggests that this argument is not as solid for short-wave radiation as for thermal radiation. Nevertheless the expectation has been confirmed experimentally in the past (e.g. Paltridge, 1974) and is again a result which emerges from the present work. (Of course it may be that the size distribution of water drops in stratocumulus is not in any event greatly variable from cloud to cloud). Equation 5a perhaps applies fairly universally for stratocumulus.

There is no such expectation for cirrus clouds since ice particles are normally much larger than 10 μm and their scattering efficiency does not change with radius. The fact that there is reasonably consistent relation (equation 5b) which fits the ice clouds of the present experiment suggests that the particle size distribution and/or the mean particle radius was fairly constant from cloud to cloud and within each cloud. Referring to Table 2, a simple calculation using the observed average particle number density and the average ice mass per unit volume puts that mean particle radius at about 200 μm. (The range over the 3 cirrus decks is about 180 to 220 μm). This figure is consistent with the size spectra and 2-D images from the Knollenberg probes. The images showed among other things that the particles were simply 'irregular' in character - there were only a very few examples of regular or repeatable shapes such as hexagonal plates or rhombic columns.

Earlier work on high cirrus cloud in New Mexico (Paltridge and Platt, 1981) yielded much higher albedo for a given ice path than is indicated by Figure 3. The simplest explanation is that the mean radius of the ice particles was smaller on that occasion. The question arises as to whether information on mean radius would allow a more universal parameterization of cirrus albedo.

A theoretical relation between albedo A and optical depth δ of a *thin non-absorbing* cloud was given by Coakley and Chýlek (1975). It is of the form

$$A = B\delta/(1 + B\delta) \tag{7}$$

where B is a parameter depending on solar zenith angle among other things. Now for a given ice path

and for large ice particles δ is proportional to the mean cross-section of the particles (see Stephens, 1978, for instance) and is thereby proportional to $1/\bar{r}_e$. Therefore

$$\delta(\bar{r}_e) = \delta(\bar{r}_o) \cdot \delta(\bar{r}_o/\bar{r}_e) \tag{8}$$

where $\bar{r}_o$ refers to the mean radius of the particles in some reference path. By inverting equation 7 so as to express $\delta(\bar{r}_o)$ in terms of an equivalent albedo $A(\bar{r}_e)$, substituting for $\delta(\bar{r}_o)$ in equation 8 and in turn for $\delta(\bar{r}_e)$ back in equation 7

$$A(\bar{r}_e) = \frac{[A_o/(1-A_o)] \cdot (\bar{r}_o/\bar{r}_e)}{1 + [A_o/(1-A_o)] \cdot (\bar{r}_o/\bar{r}_e)} \tag{9}$$

where A_o is a shortened symbol for $A(\bar{r}_o)$. Equation 9 allows one to calculate the albedo of a cirrus deck as a function of mean particle radius. *It assumes that equation 7 applies (or can be 'forced' to apply) to thick clouds.* It is therefore not a mechanistic parameterization, but is simply a convenient mathematical form which (hopefully) yields results whose accuracy is at least compatible with that of the medium definition (cloud amount and water path) of climate models. It can be used in conjunction with the experimental relation of equation 5b (which is assumed to apply to cirrus particles where $\bar{r}_e$ is 200 μm) to generate a family of albedo versus ice path curves where each curve corresponds to a given $\bar{r}_e$. This has been done in Figure 4.

There is very little other information which can be used as a check on the validity of the predicted curves of Figure 4. Referring again to the work of Paltridge and Platt on New Mexico cirrus, the

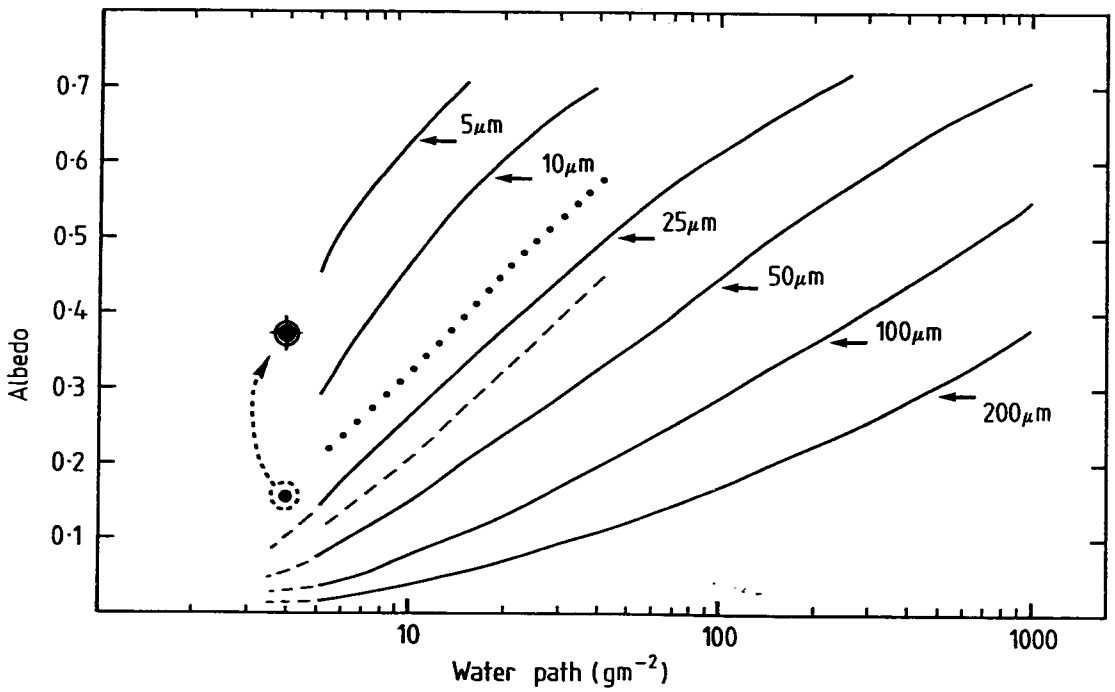

Figure (4). Total short-wave albedo for ice clouds as a function of ice-water path for various values of mean effective particle radius. The large crossed dot is the expected albedo at a water path of 4 gm^{-2} if all the water drops of a stratocumulus were transformed into equivalent irregular ice particles (see text). The dashed curve is the relation obtained in an earlier experiment on New Mexico cirrus where the solar zenith angle was about 35°. The dotted curve is that relation adjusted to take account of the higher solar zenith angle of the present work. Note that the mean particle radii of the New Mexico cirrus was of the order of 17 to 20 μm.

dashed curve of Figure 4 is the albedo versus water path relation they obtained on that occasion from three decks. The solar zenith angle at the time of the measurements was roughly 35^o. The dotted curve on Figure 4 is the same relation adjusted to bring it into line with the higher solar zenith angles ($\approx 60^o$) of the present work. The adjustment has been done according to the albedo versus solar elevation theoretical curves of Stephens (1978).

The three New Mexico decks had mean particle radii ranging from 17 to 20 μm which, bearing in mind the inherent error in this sort of measurement, are in quite remarkable agreement with the prediction of Figure 4. Note, incidentally, that the much smaller radii of the particles of the New Mexico cirrus support the work of Heymsfield and Platt (1984) on the relation between particle size and cloud temperature.

Some support to Figure 4 is given also by reference to the albedo versus *liquid* water path of equation 5a. Both theory and experiment (Platt *et al*, 1980) indicates that the albedo of cirrus is greater than that of the equivalent cloud whose particles were exactly spherical.

This is because the phase function of irregular particles is less peaked in the forward and backward direction and has greater amplitude in the 'side' directions than the equivalent spheres. The increase in albedo of irregular cirrus particles at a solar zenith angle of 60 degrees (i.e. roughly the solar zenith angle of the present measurements) can be more than a factor of 2. One can turn the argument round and say that if the water drops of stratocumulus were suddenly transformed into irregular ice particles, then the albedo would increase. The circled dot, arrow and crossed dot on Figure 4 is the change in albedo to be expected on the basis of the results of Platt *et al.* (1980) for a cloud with an initial albedo of 0.15. The increased albedo lies close to the predicted curve for irregular particles of 5 μm radius. This radius is slightly larger but of the same order as the typical radius of the water drops of stratocumulus.

If one accepts the parameterization of albedo as indicated by equations 5a and 5b and the subsequent development of equation 9, it must be emphasized again that it is derived from measurements taken over a fairly narrow range of solar zenith angles about 60 degrees. There is a theoretical basis for modifying the liquid water (i.e. spherical drop) relation of equation 5a to include a function of solar angle (e.g. Stephens, 1978), but it is an assumption (and note that it is an assumption used above) that such a modification is appropriate for cirrus clouds. It may be worth mentioning that 60^o solar zenith angle is in many cases a fair average of the solar zenith angles over a day.

Acknowledgements

Tanks are due to all members of the ASPIRE experiment team. In particular the author is indebted to Drs. C. M. R. Platt, J. C. Scott and W. King for their invaluable help and advice.

REFERENCES

Chýlek, P., 1978: Extinction and liquid water content of fogs and clouds. *J. Atmos. Sci., 35,* 296-300.

Coakley, J. A., JR., and P. Chýlek, 1975: The two stream approximation in radiative transfer: Including the angle of the incident radiation. *J. Atmos. Sci., 32,* 409-418.

Hale, G. M. and M. R. Query, 1973: Optical constants of water in the 200 nm to 200 μm wavelength region. *Appl. Opt. 12,* 555-563.

Heymsfield, A.J and C. M. R. Platt, 1984: A parameterization of the particle size spectrum of ice clouds in terms of ambient temperature and ice water content. *J. Atmos. Sci., 41,* 846-855.

Irvine, W. M. and J. B. Pollack, 1968: Infrared optical properties of water and ice spheres. *Icarus, 8,* 324-360.

King, W. D., D. A. Parkin and R. J. Handsworth, 1978: A hot-wire device having fully calculable response characteristics. *J. Appl. Meteor., 17,* 1809-1813.

King, W. D., J. E. Dye and J. W. Strapp, 1985: Icing wind tunnel tests on the CSIRO liquid water probe. *J. Atmos. Ocean. Tech., 2,* 340-352.

King, W. D. and D. E. Turvey, 1986: Thermal device for aircraft measurement of the solid water content of clouds. *J. Atmos. and Ocean. Tech.,* to be published, September 1986.

Paltridge, G. W., 1974: Infrared emissivity, Short-wave albedo, and the microphysics of Stratiform water clouds. *J. Geophys. Res., 79,* 4053-4058.

Paltridge, G. W., and C. M. R. Platt, 1981: Aircraft measurements of solar and infrared radiation and the microphysics of cirrus cloud. *Quart. J. Roy. Meteor. Soc., 107,* 367-380.

Platt, C. M. R., D. W. Reynolds and N. L. Abshire, 1980: Satellite and lidar observations of the albedo, emittance and optical depth of cirrus compared to model calculations. *Mon. Wea. Rev., 108,* 195-204.

Scott, J. D. and G. L. Stephens, 1985: A visible-infrared spectroradiometer for cloud reflectance measurements. *J. Phys. E: Sci. Instrum., 18,* 697-701.

Stephens, G. L., 1978: Radiation profiles in extended water clouds, parts I, II and III. *J. Atmos. Sci., 35,* 2111-2141.

Wiscombe, W. J., R. M. Welch and W. D. Hall, 1984: The effects of very large drops on cloud absorption. Part I: Parcel Models. *J. Atmos. Sci., 41,* 1336-1355.